Journal of Hydrology 540 (2016) 379–385

Contents lists available at ScienceDirect

Journal of Hydrology

journal homepage: www.elsevier.com/locate/jhydrol

Research papers

Long-term agricultural non-point source pollution loading dynamics and correlation with outlet sediment geochemistry

Wei Ouyang [a,*], Wei Jiao [a], Xiaoming Li [a], Elisa Giubilato [b], Andrea Critto [b]

[a] State Key Laboratory of Water Environment Simulation, School of Environment, Beijing Normal University, Beijing 100875, China
[b] Department of Environmental Sciences, Informatics and Statistics, Ca' Foscari University of Venice, Venice 30123, Italy

ARTICLE INFO

Article history:
Received 16 December 2015
Received in revised form 7 May 2016
Accepted 19 June 2016
Available online 21 June 2016
This manuscript was handled by Laurent Charlet, Editor-in-Chief, with the assistance of Fereidoun Rezanezhad, Associate Editor

Keywords:
Agricultural non-point source pollution
Sediment core
^{210}Pb
Heavy metals
Watershed water quality

ABSTRACT

Some agricultural non-point source (NPS) pollutants accumulate in sediments in the outlet sections of watersheds. It is crucial to evaluate the historical interactions between sediment properties and watershed NPS loading. Therefore, a sediment core from the outlet of an agricultural watershed was collected. The core age was dated using the ^{210}Pb method, and sedimentation rates were determined using the constant rate of supply (CRS) model. The total nitrogen (TN), total phosphorus (TP), Cd, Pb, Cu, Ni and Cr accumulations in the sediment generally showed fluctuating increases, with the highest sedimentation fluxes all occurring in approximately 1998. The measurement of specific mass sedimentation rates reflected a record of watershed soil erosion dynamics. Using SWAT (Soil and Water Assessment Tool) to simulate long-term watershed agricultural NPS pollution loadings, the historical interactions between sediment properties and NPS loadings were further evaluated. The N leaching process weakened these interactions, but the historical accumulations of TP and heavy metals in sediments generally correlated well with watershed NPS TP loading. The regression analysis suggested that Pb and Cr were the most suitable indexes for assessing long-term NPS TN and TP pollution, respectively. Assessing the NPS loading dynamics using the vertical characteristics of sediment geochemistry is a new method.

1. Introduction

Sedimentation processes usually occur during the transport of various pollutants into surface waters (Ansari et al., 2000). Consequently, sediment geochemistry is considered a useful indicator of environmental changes and anthropogenic impacts (Chatterjee et al., 2007; Nath et al., 2000). It has been widely recognized that intensive agricultural development can increase the watershed soil erosion load and release more associated non-point source (NPS) pollutants, such as nitrogen, phosphorus and heavy metals (Jain, 2002; Jiao et al., 2014). Some NPS nitrogen (N) and phosphorus (P) discharged by upland processes accumulate in river sediments. Although some fine particles are lost during the sedimentation process, it is hypothesized that some characteristics of the vertical sediment geochemistry are correlated with the NPS loading history (Migani et al., 2015). Research regarding the sediment property responses to long-term agricultural NPS pollution dynamics remains scarce.

Over the past few decades, the study of sediment cores has proven to be an excellent approach for establishing the effects of anthropogenic and natural processes on the sedimentary environment (Shotyk, 2002). Vertical profiles of pollutant species in sediment cores are commonly used as "historical pollution records" of whole watersheds (Harikumar and Nasir, 2010). To inversely identify the pollution history, it is essential to estimate the sedimentation rates and sediment ages. The results also provide valuable information regarding the soil erosion dynamics of a watershed (Mabit et al., 2014), which are directly related to agricultural NPS pollution. In this context, the application of radiometric methods to sedimentary chronology has developed rapidly and with considerable success (Kumara et al., 1999). In particular, the half-life of ^{210}Pb (22.3 years) makes it an ideal radioisotope for dating sediments from the past 100–150 years. To date, this method has been used extensively in different sedimentary environments, including wetlands, lakes, reservoirs, flood plains, estuaries and coastal areas (Mabit et al., 2014).

Effective control of NPS pollution in agricultural watersheds is required to meet the high standards of water management. Consequently, studies seeking a better understanding of watershed management have expressed increasing concern regarding the quantification of NPS pollutant loading (Dechmi and Skhiri, 2013; Heathwaite et al., 2005). Thus, a number of water quality models at the watershed scale have been developed and applied. Among

* Corresponding author.
E-mail address: wei@itc.nl (W. Ouyang).

http://dx.doi.org/10.1016/j.jhydrol.2016.06.043
0022-1694/

these models, the Soil and Water Assessment Tool (SWAT) is frequently used to assess NPS pollution over long timescales and at diverse spatial scales in agricultural watersheds (Laurent and Ruelland, 2011; Ouyang et al., 2010). However, the modeling methods are usually quite time consuming due to the input database import and parameter validation processes (Choi and Blood, 1999). Using sediment geochemistry to indicate agricultural NPS pollution is a potential way to provide the knowledge needed to support routine management, especially in data-sparse or ungauged watersheds.

Watershed sediment analyses are widely accepted indicators of environmental water quality (Somura et al., 2012). Based on the hypothesis of the interaction between sediment and NPS pollution loading, we present a new approach to validate sediment geochemistry indicators that can function on long-time scales. The interaction principle was achieved by integrating SWAT modeling and a ^{210}Pb-dated sediment analysis. The primary objectives of this study were as follows: (1) to analyze and date the total nitrogen (TN), total phosphorus (TP), Cd, Pb, Cu, Ni and Cr accumulations in sediment at a watershed outlet; (2); to identify the long-term NPS nitrogen and phosphorus loading in an agricultural watershed; and (3) to evaluate the historical interactions between sediment properties and watershed NPS TN and TP loading, thus, identifying the proper indicators.

2. Materials and methods

2.1. Study area description

The study area is located on the Sanjiang Plain, Northeast China, encompassing a total watershed area of 24,863 km^2 (Fig. 1). In addition to intensive regional agricultural development, approximately half of the natural wetlands, forests and grasslands have been reclaimed and converted into paddy land and upland since the 1950s. Rice and maize are the two main types of crops being cultivated. This watershed has a frigid, temperate, continental monsoon climate, with an average annual temperature of 1.91 °C. The mean annual precipitation is approximately 600 mm, most of which falls between May and September (Ouyang et al., 2014). The local river, with pH values ranging from approximately 0.5 to 7.1, is characterized by a seasonal hydrological regime, generally flowing from southwest to northeast.

2.2. Watershed NPS total nitrogen and phosphorus loading simulations

The SWAT model was applied to estimate watershed NPS TN and TP loads from 1977 to 2013. NPS nitrogen (N) was simulated in ammonia, organic and nitrate forms, and their sum represented the total N (TN). NPS phosphorus (P) was modeled in organic, soluble and sediment forms, and their sum represented the total P (TP). The SWAT databases were prepared and imported; including topography (1:250,000); land cover in 1979, 1992, 1999 and 2009 (1:1,000,000); climate information; and soil properties (1:1,000,000) (Fig. 1). The climatic features include daily historical monitoring data (minimum and maximum temperature, wind speed, precipitation and solar radiation) obtained from three local weather stations between 1973 and 2015. After field investigations, the agricultural practices of paddy rice and maize over three decades were taken into account to improve the modeling efficiency (Ouyang et al., 2013).

After a sensitivity analysis using the SWAT-CUP tool, the SWAT model was calibrated with monitoring data obtained in the first twenty-four months and later validated with data from an additional two years. The model was validated based on the order of streamflow and soil concentrations (Fig. 2). Using the streamflow and sediment yield routing and monitoring data, the sixteen dominant parameters (CN_2.mgt, SMTMP.bsn, ALPHA_BF.gw, TIMP.bsn, GW_DELAY.gw, CMN.bsn, CH_N_2.rte, NPERCO.bsn, CH_K_2.rte, Spexp.bsn, SOL_AWC(1-2).sol, SPCON.bsn, SOL_BD(1).sol, RSDCO.bsn, CANMX.hru, AI1.wwq, ESCO.hru, BC1.swq, GWQMN.gw, BC2.swq and BC3.swq) that affect these two indicators were validated (Fig. 3). The modeling performances of the streamflow and sediment were evaluated using the coefficient of determination (R^2) and the Nash-Sutcliffe efficiency (E_{NS}), which was larger than 0.698. The watershed NPS N and P loadings were validated with the defined parameter values due to the lack of stable nutrient concentration monitoring data. The validated parameters associated with TN and TP (Cmn, Psp, Pperco, Phoskd, BC1, BC2, BC3, BC4, AI1, AI2 and Rsdco) were predefined according to data in a similar watershed. Details of the SWAT validation process in this watershed can be found in our earlier paper (Ouyang et al., 2014). Linear

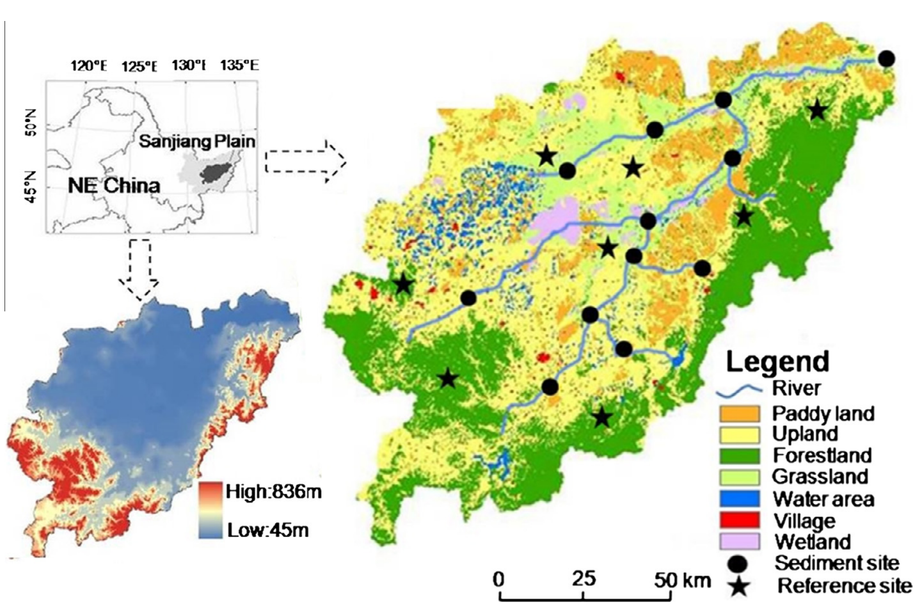

Fig. 1. Location of study area showing topography, land uses and sampling sites.

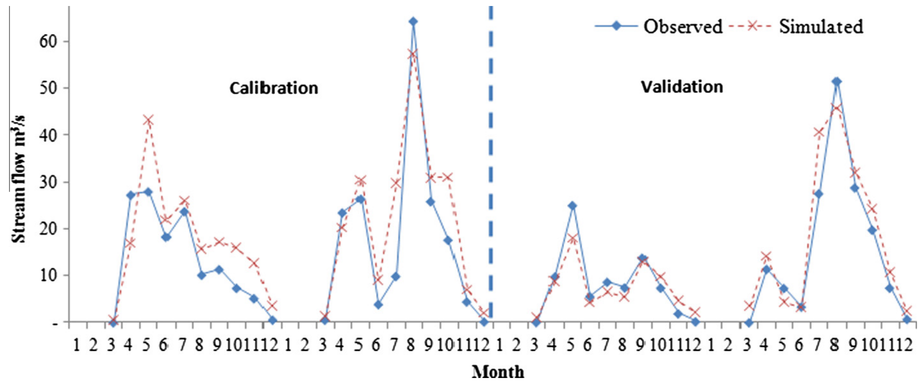

Fig. 2. Calibration and validation of the streamflow.

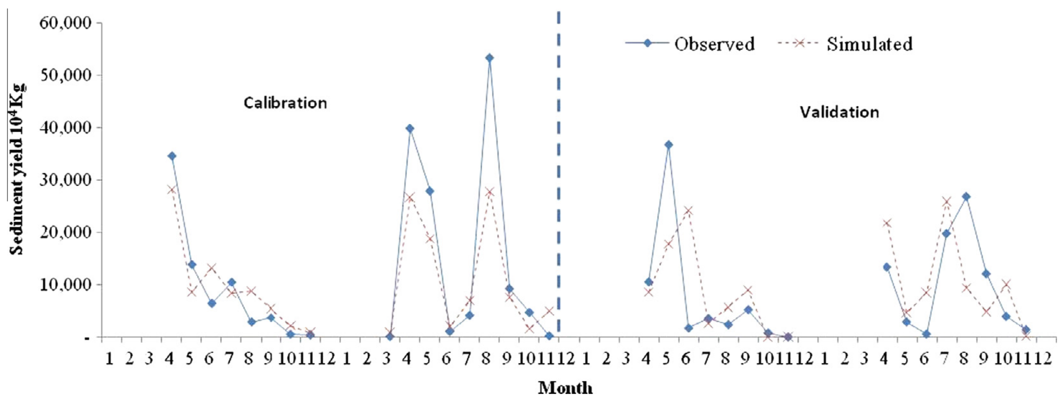

Fig. 3. Calibration and validation of the sand concentration.

regressions between the watershed NPS TN and TP loadings in each year and the dated sediment cores can also be used as assessment indicators for model validation.

2.3. Watershed outlet sediment coring and pretreatment

At the watershed outlet section, a 40 cm long and 4 cm diameter river sediment core was collected in July 2013 (Fig. 1). During the coring process, special care was taken to ensure minimum disturbance of the sediment-water interface. The gravity-coring unit was lowered as slowly as possible into the sediment to avoid lateral movements, which are caused by the pressure wave created by the descent of the corer. After collection, the sediment core was sliced at 1 cm intervals from top to bottom. All the sliced layers were sealed in polyethylene bags and transported to the laboratory immediately. There, they were air dried at room temperature, ground with a pestle and mortar (XPM-120x3, China) and passed through a 100-mesh nylon sieve.

2.4. Sediment total nitrogen, phosphorus and heavy metal concentration analyses

To identify the sediment geochemical variability under long-term agricultural development, we analyzed the total nitrogen (TN), total phosphorus (TP), Cd, Pb, Cu, Ni and Cr concentrations in each sediment sample. These parameters were sensitive during tillage practices. TN was measured directly using a CHN Elemental Analyzer. To analyze TP and heavy metal concentrations, sediment samples were digested with an acid mixture of HF-HNO_3-$HClO_4$ and measured using inductively coupled plasma-atomic emission

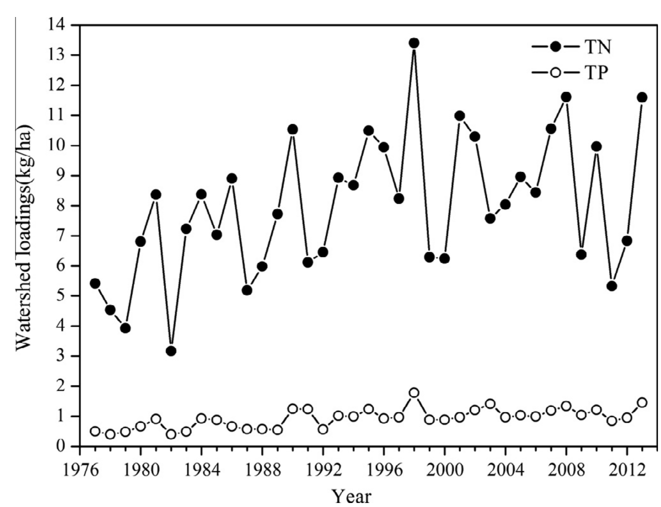

Fig. 4. Long-term watershed NPS total nitrogen and phosphorus loadings.

spectroscopy (ICP-AES) (IRIS Intrepid II XSP, Thermo Electron, USA).

2.5. ^{210}Pb activity and sedimentation rate determination

The chronology of the sediment core was determined using the ^{210}Pb method and high-resolution gamma ray spectrometry with an HPGe detector (HPGe GWL series, ORTEC, USA). There are two sources of ^{210}Pb found in sediments: in situ decay of ^{226}Ra, also called supported ($^{210}Pb_{sup}$), and natural fallout (Krishnaswamy

Table 1
Total, supported and excess ^{210}Pb activities and CRS-modeled sedimentation rates.

Depth (cm)	$^{210}Pb_{tot}$ (Bg/kg)	$^{210}Pb_{sup}$ (Bg/kg)	$^{210}Pb_{ex}$ (Bg/kg)	Mass rate (mg/cm^2 a)	Linear rate (cm/a)	Sedimentation date (Year)
0–1	28.56	14.37	14.19	497.71	0.62	2013
1–2	28.64	14.89	13.75	488.18	0.60	
2–3	27.34	14.75	12.59	504.82	0.60	2008
3–4	26.38	13.95	12.43	484.76	0.55	
4–5	27.49	16.25	11.24	506.16	0.60	2003
5–6	25.68	15.01	10.67	504.71	0.58	
6–7	24.17	14.42	9.75	523.15	0.59	1998
7–8	24.30	14.72	9.58	504.16	0.59	
8–9	23.59	14.54	9.05	505.47	0.60	1993
9–10	21.70	13.31	8.39	516.41	0.61	
10–11	24.02	15.82	8.20	501.66	0.58	1988
11–12	21.21	13.69	7.52	519.00	0.61	
12–13	22.69	15.40	7.29	506.34	0.57	1983
13–14	21.52	14.12	7.40	472.15	0.53	
14–15	21.03	14.02	7.01	469.77	0.53	1978
15–16	23.21	16.43	6.78	453.36	0.48	
16–17	22.02	15.61	6.41	452.50	0.49	1973
17–18	22.71	16.41	6.30	430.03	0.45	
18–19	19.68	13.79	5.89	427.52	0.44	1968
19–20	20.29	15.11	5.18	449.13	0.47	
20–21	21.91	16.97	4.94	444.86	0.46	1963
21–22	21.04	16.13	4.91	419.44	0.42	
22–23	19.39	14.80	4.59	412.94	0.41	1958
23–24	20.50	16.31	4.19	415.20	0.42	
24–25	18.90	14.80	4.10	394.95	0.39	1953
25–26	20.12	16.11	4.01	373.68	0.36	
26–27	20.28	16.31	3.97	342.54	0.32	1948
27–28	18.58	14.78	3.80	319.59	0.31	
28–29	18.56	15.25	3.31	330.27	0.32	1943
29–30	18.97	15.56	3.41	293.08	0.26	
30–31	18.50	15.61	2.89	300.66	0.27	1938
31–32	19.00	16.21	2.79	278.04	0.25	
32–33	18.20	15.52	2.68	253.73	0.22	1933
33–34	19.18	16.68	2.50	236.66	0.20	
34–35	18.51	16.00	2.51	199.30	0.17	1928
35–36	18.80	16.58	2.22	184.01	0.16	
36–37	17.83	15.92	1.91	163.04	0.12	1923
37–38	16.97	14.97	2.00	124.56	0.09	
38–39	17.52	15.68	1.84	89.70	0.06	1918
39–40	17.43	15.62	1.81	45.86	0.04	

et al., 1971). Consequently, the total activity of this isotope ($^{210}Pb_{tot}$) in sediments is the sum of supported ($^{210}Pb_{sup}$) and atmospherically derived ^{210}Pb. The latter term, called unsupported or excess ($^{210}Pb_{ex}$), can be obtained by subtracting the measured activity in secular equilibrium with ^{226}Ra from $^{210}Pb_{tot}$ in each sediment sample (San Miguel et al., 2004). After a month of storage in sealed containers to allow radioactive equilibration, $^{210}Pb_{tot}$ was determined from the 46.5-keV gamma ray emissions, and ^{226}Ra was determined from the 295.2-keV and 351.9-keV gamma rays emitted by its daughter isotope ^{214}Pb. The precision of this analytical method was usually higher than 10%. To help date the sediment core, sedimentation rates were estimated using the constant rate supply (CRS) model, which assumes a constant rate of $^{210}Pb_{ex}$ from atmospheric fallout but allows sediment accumulation to vary (Appleby and Oldfield, 1978).

2.6. Statistical analysis

The vertical concentrations of TN, TP and heavy metals in sediments were dated based on the ^{210}Pb pattern in the sediment core from the outlet section. Then, the corresponding simulated agricultural NPS pollution at the same temporal scale was correlated with the vertical distributions of TN, TP and heavy metal concentrations. The other eleven sediment samples were used to identify the anthropogenic sources of heavy metals in this watershed (Jiao et al., 2015). The entire statistical analysis was carried out in Origin Software.

3. Results

3.1. Long-term watershed NPS total nitrogen and phosphorus loadings

The watershed NPS TN and TP loadings were simulated with SWAT model from 1977 to 2013 (Fig. 4). The watershed NPS nutrient pollution generally displayed strong variability throughout the period. The TN loadings ranged from 3.17 to 13.41 kg/ha, with an annual average of 7.92 kg/ha. The TP loadings ranged from 0.40 to 1.78 kg/ha, with an annual average of 0.95 kg/ha. The highest TN and TP loadings occurred in 1998, which were 1.69 and 1.87 times larger than the simulated annual averages, respectively. These results were in agreement with the highest accumulation fluxes in 1998 at a sediment depth of 7 cm, indicating that the CRS-modeled dates, at least in the upper part of the core, were reasonable.

3.2. Watershed outlet sedimentation rates and age dating

The total, supported and excess ^{210}Pb activities and CRS-modeled sedimentation rates are shown in Table 1 as functions of sediment depth. In general, the $^{210}Pb_{tot}$ activities varied significantly from 16.97 to 28.64 Bg/kg, with an average activity of 21.41 Bg/kg. However, the $^{210}Pb_{sup}$ activities were relatively constant and ranged between 13.30 and 16.97 Bg/kg. The $^{210}Pb_{ex}$ activities were calculated as the difference between $^{210}Pb_{tot}$ and $^{210}Pb_{sup}$, which reached its maximum of 14.19 Bg/kg in the surface sediment. The $^{210}Pb_{ex}$ activities generally showed an almost monotonic decline with sediment depth. This decline indicated a rather undisturbed sediment core environment, where bioturbation or physical mixing could be considered negligible. According to the CRS modeling results, the watershed mass sedimentation rates ranged from 45.86 to 523.15 mg/cm^2 a, with an average linear rate of 0.40 cm/a. Therefore, if the linear rate was maintained, the 40 cm sediment core actually spanned a period from 1913 to 2013.

3.3. Total nitrogen and phosphorus accumulations in the sediment core

To consider the sedimentation rate variation over the period, the TN and TP fluxes to the sediment core were calculated by multiplying their concentrations by the CRS-modeled mass sedimentation rate in each analyzed layer. Because this watershed has experienced extensive agricultural reclamation since the 1950s, the sedimentation fluxes in this period exhibited slight increasing patterns due to the disturbances of tillage practices and land use conversion (Fig. 5). During the same period, the watershed NPS TN and TP accumulations in sediments generally showed a fluctuating, increasing trend, with the highest sedimentation fluxes occurring in approximately 1998. The TN fluxes ranged from 222.43 to 313.89 μg/cm^2 a, with an average of 280.17 μg/cm^2 a. The TP fluxes were generally low before 1988, but exceeded TN fluxes after 1988, averaging 288.64 μg/cm^2 a. By comparison, the watershed TN sedimentation fluxes showed much weaker historical variability than did TP fluxes, especially recently.

3.4. Heavy metal accumulations in the sediment core

Following the same flow chart, the Cd, Pb, Cu, Ni and Cr fluxes into the sediment core from 1948 to 2013 are also illustrated in Fig. 6. The sedimentation fluxes of these heavy metals fluctuated and exhibited an increasing trend. Cd ranged from 0.04 to 0.16 μg/cm^2 a, with the average flux of 0.09 μg/cm^2 a. Pb ranged from 6.38 to 10.14 μg/cm^2 a, with the average flux of 8.31 μg/cm^2 a. Cu ranged from 6.70 to 11.50 μg/cm^2 a, with an average flux of 8.99 μg/cm^2 a. Ni ranged from 8.78 to 14.40 μg/cm^2 a, with an average flux of 11.87 μg/cm^2 a. Cr ranged from 21.00 to 31.99 μg/cm^2 a, with an average flux of 25.26 μg/cm^2 a. For all heavy metals, the highest sedimentation fluxes occurred in 1998, suggesting that their watershed release histories are similar to those of TN and TP.

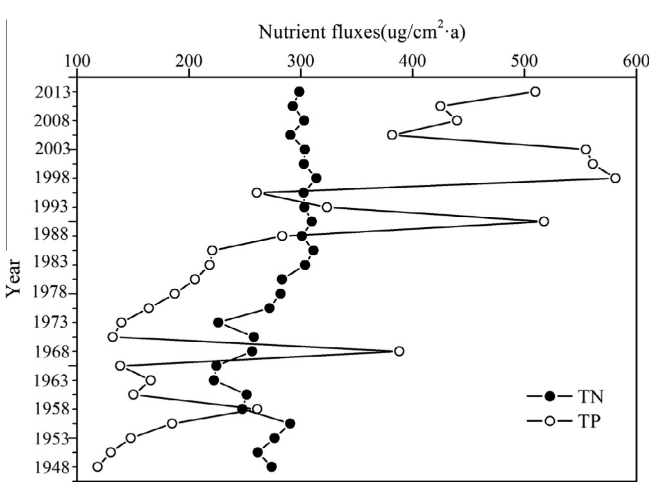

Fig. 5. Historical accumulations of TN and TP in the sediment core.

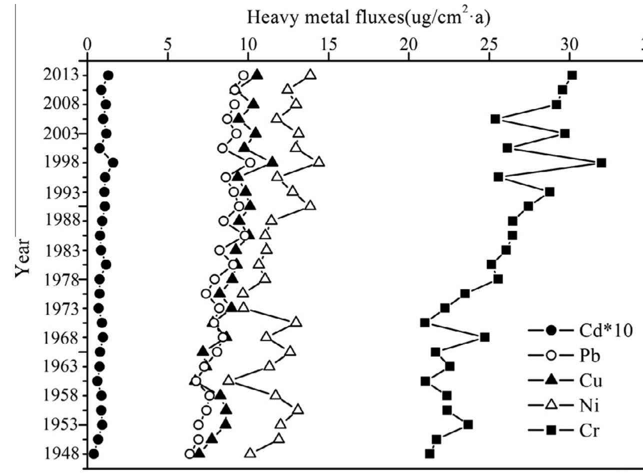

Fig. 6. Historical accumulations of heavy metals in the sediment core.

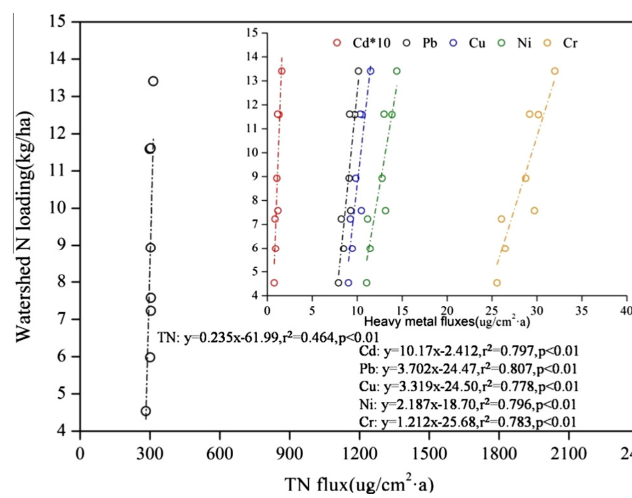

Fig. 7. Relationships between simulated watershed NPS total nitrogen loading and TN and heavy metal fluxes from the sediment analysis.

3.5. Relationships between NPS nitrogen and phosphorus and sediment properties

After obtaining the long-term NPS TN and TP loadings, a regression analysis was applied to assess their relationships with watershed sedimentation fluxes in 2013, 2008, 2003, 1998, 1993, 1988, 1983 and 1978 (Fig. 7). The sedimentation flux of TN generally showed a positive relationship with watershed NPS loading, with an R^2 value of 0.464. However, the relationship was much weaker when compared to Cd, Pb, Cu, Ni and Cr. These results clearly suggest that the accumulations of heavy metals in sediments were more sensitive to NPS nitrogen pollution. By comparing the fitting lines, Pb had a higher R^2 value than those of other heavy metals. Therefore, it can be selected as the best sediment index to assess long-term watershed NPS TN loading.

The historical relationships between NPS TP loading and watershed sedimentation fluxes are shown in Fig. 8. Compared to responses to watershed NPS nitrogen pollution, the sediment property responses to NPS phosphorus pollution were much stronger.

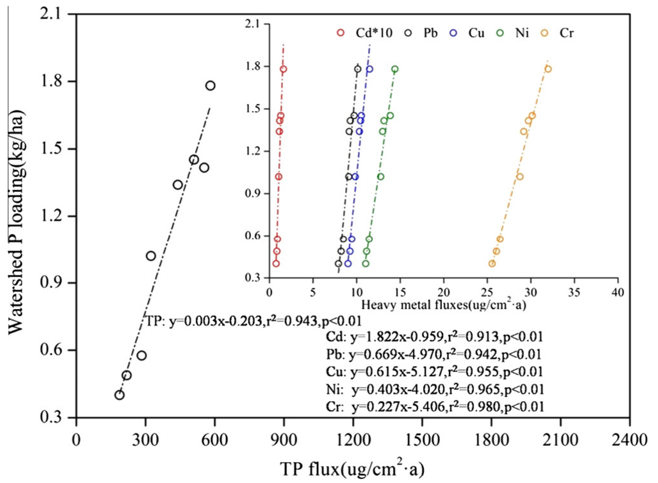

Fig. 8. Relationships between simulated watershed NPS total phosphorus loading with TP and heavy metal fluxes from the sediment analysis.

In general, the TP sedimentation flux correlated well with NPS loading, with an R^2 value of 0.943. The large value suggests that the sediment properties at the outlet can clearly express NPS phosphorus loading. Based on the high R^2 values of Cu, Ni and Cr, these heavy metals were the best stable indicators. Among these heavy metals, Cr was found to provide the most reliable information regarding watershed NPS TP pollution.

4. Discussion

4.1. Historical interactions between sediment properties and long term NPS pollution loading

To evaluate the historical interactions between sediment properties and NPS pollution, the watershed NPS TN and TP loadings were simulated using SWAT from 1977 to 2013 (Fig. 4). The NPS pollution loadings display strong temporal variability throughout the period. However, the TN fluxes in sediments remained relatively stable in recent years, which disagreed with the simulation results. A potential explanation for this result is that leaching occurred after N deposition in the sediments, and NPS nitrogen pollution mainly occurs in soluble form (Almasri and Kaluarachchi, 2007). Conversely, the accumulations of heavy metals in sediments are found to be more sensitive to watershed NPS nitrogen pollution. By comparing the fitting lines, Pb had a higher R^2 value than those of TN and other heavy metals. Therefore, it is selected as the most accurate sediment index used to indicate long-term NPS TN pollution.

When compared to watershed NPS TN pollution, the NPS TP loading was found to be a much lower load throughout the simulation period. A previous study indicated that even slight changes in NPS phosphorus pollution loading can considerably affect water quality in agricultural watersheds (Tesoriero et al., 2009). By comparison, the TP fluxes exhibited stronger variability in sediments and exceeded TN fluxes after approximately 1988 (Fig. 6). Because the formation and transport of NPS phosphorus occur mainly in particulate form (Leone et al., 2008), historical accumulation of TP in sediments generally correlated well with watershed NPS loading, with an R^2 value of 0.943. However, this value is still lower than those of heavy metals such as Cu, Ni and Cr. Among these heavy metals, Cr mainly stems from an anthropogenic source due to phosphorus fertilizers (Ouyang et al., 2012) and can provide reliable information to assess NPS TP pollution.

4.2. Watershed outlet sediment geochemical variability with long-term agricultural development

Intensive agricultural activities impact ecological and environmental quality and affect water quality (Hosono et al., 2007). One of the most significant impacts is from increased NPS pollution loading, which has caused serious water pollution problems in recent decades (Zia et al., 2013). In this study, the impact of long-term agricultural development on the watershed environment was evaluated by analyzing a river sediment core from an outlet section. The watershed TN, TP and heavy metals accumulations in sediments generally showed fluctuating increases during long-term agricultural development (Figs. 4 and 5). Such sediment geochemical variability is in agreement with the results of case studies in other watersheds in China, suggesting the existence of continuously growing environmental and hydrological pressure (Tang et al., 2010; Wang et al., 2004).

It is widely accepted that frequent tillage activities can accelerate soil erosion, which has a close relationship with watershed sediment geochemistry (Quinton and Catt, 2007). Measurements of specific mass sedimentation rates reflect a historical record of watershed soil erosion processes. According to the CRS model results, the studied watershed had an average sedimentation rate of 472.18 mg/cm^2 a from 1953 to 2013 (Table 1). This rate is much higher in the latter portion of the period, highlighting the temporal effects of long-term cultivation. However, abrupt changes in the mass sedimentation rate and TN, TP and heavy metal fluxes occur in approximately 1998. This can be attributed to an extreme flood in this year because the watershed soil erosion dynamics are also determined by natural hydrology (Oeurng et al., 2010). By comparison, the sedimentation rates were almost constant after 2008, but the sedimentation fluxes of TP and heavy metals still exhibit obvious increasing trends. With growing concern regarding environmental protection, some soil and water conservation measures have been gradually implemented in recent years. However, the amount of phosphate fertilizer usage also increased to produce higher crop yields, reaching 87 kg P/ha in 2010 (Jiao et al., 2014). Therefore, the excessive application of phosphorus fertilizers that contain a variety of trace metals and impurities may be the major cause of recent sediment geochemical variability.

4.3. Implications for watershed NPS nitrogen and phosphorus control

With continuous industrial emission controls, agricultural NPS has been increasingly recognized as a major contributor to watershed nitrogen and phosphorus pollution (Dupas et al., 2015). Consequently, assessments of agricultural NPS loading are becoming more important when formulating effective watershed management strategies (Rao et al., 2009). This study proved the hypothesis regarding the link between sediment geochemistry with historical NPS pollution loading. The approach demonstrated that overall sediment geochemistry information can be used to assess long-term NPS TN and TP pollution before applying complicated models. Sediment analysis is also a potential method for model validation in ungauged watersheds. However, this approach better indicated watershed NPS phosphorus pollution.

The leaching process weakened the historical interactions between sediment properties and watershed NPS TN loading. Therefore, further attention should be paid to soil water leaching when implementing effective NPS nitrogen controls. In agricultural watersheds, soil heavy metals tend to enter the aquatic environment together with various nutrient pollutants (Yang et al., 2013). Because heavy metals deposited in sediments are not biodegradable, they are better tracers of watershed nutrient pollution compared to using nutrient indexes alone (Jin et al., 2010). The regression analyses suggest that Pb and Cr are the most suitable indexes for assessing long-term NPS TN and TP pollution, respectively.

5. Conclusions

This study proved the hypothesis that watershed agricultural NPS pollution loading is closely correlated with watershed outlet sediment geochemistry patterns. The historical interactions between sediment properties and NPS TN and TP pollution were further evaluated. This approach can be used to indicate long-term NPS pollution dynamics. The historical accumulations of TP and heavy metals in sediments generally correlated well with watershed NPS TP loading. The regression analysis suggested that Pb and Cr were the most suitable indexes for assessing long-term NPS nutrient pollution.

By analyzing the river sediment core at the watershed outlet, it was found that the watershed TN, TP, Cd, Pb, Cu, Ni and Cr accumulations in sediments showed fluctuating, increasing trends. According to the CRS results, the watershed had an average mass sedimentation rate of 472.18 mg/cm^2 a from 1953 to 2013. This value was higher earlier in the period, highlighting the influence of long-term cultivation. Abrupt changes in the mass sedimentation rate and TN, TP and heavy metal fluxes occurred in approximately 1998 due to an extreme flood. By comparison, the watershed sedimentation rates were almost constant after 2008, but the sedimentation fluxes of TP and heavy metals still exhibited increasing trends due to the excessive application of phosphorus fertilizers.

Acknowledgements

This work was financially supported by the National Natural Science Foundation of China (Grant No. 41371018), the Supporting Program of the "Twelfth Five-year Plan" for Science & Technology Research of China (2012BAD15B05) and the European Union Seventh Framework Programme (FP7/2007-2013) under Grant Agreement No. 269233–GLOCOM (Global Partners in Contaminated Land Management).

References

Almasri, M.N., Kaluarachchi, J.J., 2007. Modeling nitrate contamination of groundwater in agricultural watersheds. J. Hydrol. 343, 211–229.
Ansari, A.A., Singh, I.B., Tobschall, H.J., 2000. Importance of geomorphology and sedimentation processes for metal dispersion in sediments and soils of the Ganga Plain: identification of geochemical domains. Chem. Geol. 162 (3–4), 245–266.
Appleby, P.G., Oldfield, F., 1978. The calculation of lead-210 dates assuming a constant rate of supply of unsupported Pb-210 in the sediment. Catena 5, 1–8.
Chatterjee, M., Silva Filho, E.V., Sarkar, S.K., Sella, S.M., Bhattacharya, A., Satpathy, K. K., Prasad, M.V.R., Chakraborty, S., Bhattacharya, B.D., 2007. Distribution and possible source of trace elements in the sediment cores of a tropical macrotidal estuary and their ecotoxicological significance. Environ. Int. 33, 346–356.
Choi, K.S., Blood, E., 1999. Modeling developed coastal watersheds with the agricultural non-point source model. J. Am. Water Resour. 35, 233–244.
Dechmi, F., Skhiri, A., 2013. Evaluation of best management practices under intensive irrigation using SWAT model. Agric. Water Manage. 123, 55–64.
Dupas, R., Delmas, M., Dorioz, J.M., Garnier, J., Moatar, F., Gascuel-Odoux, C., 2015. Assessing the impact of agricultural pressures on N and P loads and eutrophication risk. Ecol. Indic. 48, 396–407.
Harikumar, P.S., Nasir, U.P., 2010. Ecotoxicological impact assessment of heavy metals in core sediments of a tropical estuary. Ecotoxicol. Environ. Saf. 73, 1742–1747.
Heathwaite, A.L., Dils, R.M., Liu, S., Carvalho, L., Brazier, R.E., Pope, L., Hughes, M., Philips, G., May, L., 2005. A tiered risk-based approach for predicting diffuse and point source phosphorus losses in agricultural areas. Sci. Total Environ. 344, 225–239.
Hosono, T., Nakano, T., Igeta, A., Tayasu, I., Tanaka, T., Yachi, S., 2007. Impact of fertilizer on a small watershed of Lake Biwa: use of sulfur and strontium isotopes in environmental diagnosis. Sci. Total Environ. 384, 342–354.
Jain, C.K., 2002. A hydro-chemical study of a mountainous watershed: the Ganga, India. Water Res. 39, 1262–1274.
Jiao, W., Ouyang, W., Hao, F.H., Huang, H.B., Shan, Y.S., Geng, X.J., 2014. Combine the soil water assessment tool (SWAT) with sediment geochemistry to evaluate diffuse heavy metal loadings at watershed scale. J. Hazard. Mater. 280, 252–259.
Jiao, W., Ouyang, W., Hao, F.H., Lin, C.Y., 2015. Anthropogenic impact on diffuse trace metal accumulation in river sediments from agricultural reclamation areas with geochemical and isotopic approaches. Sci. Total Environ. 536, 609–615.
Jin, Z.D., Cheng, H.X., Chen, L., Li, X.D., Zhu, G.W., Zhuang, G.M., Qian, N., 2010. Concentrations and contamination trends of heavy metals in the sediment cores of Taihu Lake, East China, and their relationship with historical eutrophication. Chin. J. Geochem. 29, 33–41.
Krishnaswamy, S., Lal, D., Martin, J.M., Meybeck, M., 1971. Geochronology of lake sediments. Earth Planet. Sci. Lett. 11 (1), 407–414.
Kumara, U.S., Navada, S.V., Rao, S.M., Nachiappan, Rm.P., Kumar, Bhishm., Krishnamoorthy, T.M., Jha, S.K., Shukla, V.K., 1999. Determination of recent sedimentation rates and pattern in Lake Naini, India by ^{210}Pb and ^{137}Cs dating techniques. Appl. Radiat. Isotopes 51, 97–105.
Laurent, F., Ruelland, D., 2011. Assessing impacts of alternative land use and agricultural practices on nitrate pollution at the catchment scale. J. Hydrol. 409, 440–450.
Leone, A., Ripa, M.N., Boccia, L., Lo Porto, A., 2008. Phosphorus export from agricultural land: a simple approach. Biosyst. Eng. 101, 270–280.
Mabit, L., Benmansour, M., Abril, J.M., Walling, D.E., Meusburger, K., Iurian, A.R., Bernard, C., Tarjan, S., Owens, P.N., Blake, W.H., Alewell, C., 2014. Fallout ^{210}Pb as a soil and sediment tracer in catchment sediment budget investigations: a review. Earth-Sci. Rev. 138, 335–351.
Migani, F., Borghesi, F., Dinelli, E., 2015. Geochemical characterization of surface sediments from the northern Adriatic wetlands around the Po river delta. Part I: Bulk composition and relation to local background. J. Geochem. Explor. 156, 72–88.
Nath, B.N., Kuzendory, H., Pluger, W.L., 2000. Influence of provenance weathering and sedimentary process on the elemental ratios of the fine-grained fractions of the bed load sediments from Vembanad Lake and the adjoining continental shelf, south west coast of India. J. Sediment. Petrol. 70, 1081–1094.
Oeurng, C., Sauvage, S., Sanchez-Perez, J.M., 2010. Dynamics of suspended sediment transport and yield in a large agricultural catchment, Southwest France. Earth Surf. Process. 35, 1289–1301.
Ouyang, W., Huang, H.B., Hao, F.H., Shan, Y.S., Guo, B.B., 2012. Evaluating spatial interaction of soil property with non-point source pollution at watershed scale: the phosphorus indicator in Northeast China. Sci. Total Environ. 432, 412–421.
Ouyang, W., Skidmore, A.K., Toxopeus, A.G., Hao, F.H., 2010. Long-term vegetation landscape pattern with non point source nutrient pollution in upper stream of Yellow River basin. J. Hydrol. 389, 373–380.
Ouyang, W., Song, K.Y., Wang, X.L., Hao, F.H., 2014. Non-point source pollution dynamics under long-term agricultural development and relationship with landscape dynamics. Ecol. Indic. 45, 579–589.
Ouyang, W., Huang, H.B., Hao, F.H., Guo, B.B., 2013. Synergistic impacts of land-use change and soil property variation on non-point source nitrogen pollution in a freeze-thaw area. J. Hydrol. 495 (12), 126–134.
Quinton, J.N., Catt, J.A., 2007. Enrichment of heavy metals in sediment resulting from soil erosion on agricultural fields. Environ. Sci. Technol. 41, 3495–3500.
Rao, N.S., Easton, Z.M., Schneiderman, E.M., Zion, M.S., Lee, D.R., Steenhuis, T.S., 2009. Modeling watershed-scale effectiveness of agricultural best management practices to reduce phosphorus loading. J. Environ. Manage. 90, 1385–1395.
San Miguel, E.G., Bolivar, J.P., Garcia-Tenorio, R., 2004. Vertical distribution of Th-isotope ratios, ^{210}Pb, ^{226}Ra and ^{137}Cs in sediment cores from an estuary affected by anthropogenic releases. Sci. Total Environ. 318, 143–157.
Shotyk, W., 2002. The chronology of anthropogenic, atmospheric Pb deposition recorded by peat cores in three minerogenic peat deposits from Switzerland. Sci. Total Environ. 292, 19–31.
Somura, H., Takeda, I., Arnold, J.G., Mori, Y., Jeong, J., Kannan, N., Hoffman, D., 2012. Impact of suspended sediment and nutrient loading from land uses against water quality in the Hii River basin, Japan. J. Hydrol. 450–451 (11), 25–35.
Tang, W.Z., Shan, B.Q., Zhang, H., Mao, Z.P., 2010. Heavy metal sources and associated risk in response to agricultural intensification in the estuarine sediments of Chaohu Lake Valley, East China. J. Hazard. Mater. 176, 945–951.
Tesoriero, A.J., Duff, J.H., Wolock, D.M., Spahr, N.E., Almendinger, J.E., 2009. Identifying pathways and processes affecting nitrate and orthophosphate inputs to streams in agricultural watersheds. J. Environ. Qual. 38, 1892–1900.
Wang, G.P., Liu, J.S., Tang, J., 2004. The long-term nutrient accumulation with respect to anthropogenic impacts in the sediments from two freshwater marshes (Xianghai Wetlands, Northeast China). Water Res. 38, 4462–4474.
Yang, Y.G., He, Z.L., Wang, Y.B., Fan, J.H., Liang, Z.B., Stoffella, P.J., 2013. Dissolved organic matter in relation to nutrients (N and P) and heavy metals in surface runoff water as affected by temporal variation and land uses – a case study from Indian River Area, south Florida, USA. Agric. Water Manage. 118, 38–49.
Zia, H., Harris, N.R., Merrett, G.V., Rivers, M., Coles, N., 2013. The impact of agricultural activities on water quality: a case for collaborative catchment-scale management using integrated wireless sensor networks. Comput. Electron. Agric. 96, 126–138.